

Layering at Free Liquid Surfaces

E. Chacón,¹ M. Reinaldo-Falagán,² E. Velasco,^{2,3} and P. Tarazona^{2,3}

¹*Instituto de Ciencia de Materiales de Madrid, Consejo Superior de Investigaciones Científicas. Cantoblanco, E-28049 Madrid, Spain*

²*Departamento de Física Teórica de la Materia Condensada, Universidad Autónoma de Madrid, E-28049 Madrid, Spain*

³*Instituto Nicolás Cabrera, Universidad Autónoma de Madrid, E-28049 Madrid, Spain*

(Received 20 March 2001; published 26 September 2001)

We show that simple liquids, with appropriate choices of the isotropic pair interaction, may exhibit surface layering above the melting temperature. Results for the liquid surface have been obtained by Monte Carlo simulations in slab geometry. Surface layering appears at temperatures below approximately one-third of the critical temperature for very different choices of pair interaction. The high melting temperature of the Lennard-Jones crystal preempts the observation of the oscillatory density at the free liquid interface, while model pair interaction potentials, built to reproduce some properties of mercury and the alkali metals, have low melting temperature, uncovering the region of surface layering.

DOI: 10.1103/PhysRevLett.87.166101

PACS numbers: 68.05.-n, 61.25.Mv, 64.70.Fx

Surface-induced order is a well-known effect in liquid crystals [1,2] and at the interface between a simple fluid and a sharp wall [3], but the effect was believed to be absent at the free surface of simple fluids with isotropic interactions, for which the density seems to decrease monotonically along the normal to the liquid-vapor interface [4]. However, the possible existence of surface atomic layering in liquid metals and semiconductors [5] has attracted much attention during the past years. Although the results were not conclusive, early experiments indicated an increased surface density for Hg [6]. This was supported by simulations [7] and theoretical studies [8] predicting strong layering at the free surface. Only recently has there been clear evidence from x-ray reflectivity of the oscillations of the longitudinal density distributions in the liquid-vapor interface of Hg [9] and Ga [10].

Still, surface layering could be common to all liquid metals or alternatively it might be due to the strong peculiarities of liquid Hg (with a metal-nonmetal transition) and liquid Ga (denser than its crystal phase which displays pseudodimerization of atoms). Rice and co-workers [7], based on self-consistent quantum Monte Carlo (MC) simulations using a pseudopotential for the electron-ion and the ion-ion interactions, claimed that the density oscillations are due to the coupling between the electronic and ionic profiles. They observed that the electron density profile decays very abruptly, generating an effective wall potential against which the ions lay orderly, much in the same way as a hard-sphere fluid next to a hard wall. Tosatti and co-workers [11] used a *glue* model to argue that many-body forces, arising from delocalized electrons in metals, tend to increase the surface density to bring the undercoordinated surface atoms to an optimal bulklike coordination. In doing so, the atoms immediately below would have a high coordination and reduce the density, creating a density oscillation that propagates into the bulk liquid. Despite their

different points of view, both explanations are based on the metallic character of the binding interactions.

In this Letter we argue that layering at free liquid surfaces may be a more universal behavior, the many-body nature of metallic interactions not playing necessarily a leading role, besides determining the shape of the effective pair potentials. Our hypothesis is that layering would be a common feature of free liquid surfaces well below the critical temperature, but that in simple fluids it is preempted by solidification, below which the liquid becomes metastable and the free liquid-vapor interface cannot be observed at equilibrium. This hypothesis agrees with the fact that both Hg and Ga have low melting points, with a ratio between melting (T_m) and critical (T_c) temperatures of $T_m/T_c = 0.13$ for Hg and even lower for Ga. Other liquid metals such as the alkalis have a ratio close to 0.15, much lower than the value (0.55) for the noble gases. The aim of this Letter is to show that there are simple pair interaction models that reproduce the low T_m/T_c ratio, typical of liquid metals, and that the free liquid surface of these models exhibits density oscillations. In order to find pair potentials with a low reduced melting temperature we started with effective model descriptions reproducing some features of the alkali metals and Hg. We used total energy local density approximation results for Na crystals, calculated as a function of the lattice constant for both bcc and fcc lattices [12], and searched for the best fit to a simple pair potential $E = \sum_{i,j} \phi(r_{ij})$, within a broad parametrized functional family for $\phi(r)$. Inverse power forms, including the Lennard-Jones (LJ) potential, could not fit crystal energies to that simple pairwise form, but we obtained an accurate fit using

$$\phi_{\text{Na}}(r) = A_0 e^{-\alpha r} - A_1 e^{-\beta(r-R_1)^2},$$

with $A_0 = 437.96$ eV, $\alpha = 2.2322 \text{ \AA}^{-1}$, $A_1 = 0.18382$ eV, $\beta = 0.214 \text{ \AA}^{-2}$, and $R_1 = 3.5344 \text{ \AA}$, so

that the exponential term describes mainly the repulsive part of the potential and the attraction is given by the Gaussian. In Fig. 1 we show this pair potential, called $\phi_{\text{Na}}(r)$ henceforth, which is quite different from a LJ potential $\phi_{\text{LJ}}(r)$ —much sharper in the repulsive part and narrower in the attractive well. The soft repulsion of our effective potential agrees with the general characteristics of alkali metal interactions [13], where the softness of the repulsion reflects the overlap of open valence levels. Note that in order to compare the different models the reduced units are defined in terms of a length which makes $\phi(\sigma) = 0$ and an energy defined as $U = -\frac{9}{8}\sigma^{-3} \int_{\sigma}^{\infty} dr r^2 \phi(r)$ to reproduce for the LJ model the usual parameters σ and $\epsilon \equiv U_{\text{LJ}}$. Our effective Na description gives the values $\sigma_{\text{Na}} = 3.48 \text{ \AA}$ and $U_{\text{Na}} = 0.1885 \text{ eV}$.

We use a fit to the results of inverting the structure factor of Hg in a hot metallic state ($T = 1273 \text{ K}$, $\rho = 10.98 \text{ g/cm}^3$) [14] to obtain the effective pair potential $\phi_{\text{Hg}}(r)$ presented in Fig. 1, with $\sigma_{\text{Hg}} = 2.91 \text{ \AA}$ and $U_{\text{Hg}} = 0.12633 \text{ eV}$. This Hg model has steeper repulsion and a flatter potential well than both the LJ and the alkalis. It must be stressed that these “Na” and “Hg” pair potentials cannot be very accurate representations of the interactions for these liquid metals, in the full range of density and temperature. They are built from a limited amount of information for each system and they are not expected to reproduce quantitatively other experimental properties. However, as will be seen below, these simple interaction models give the qualitative features of low

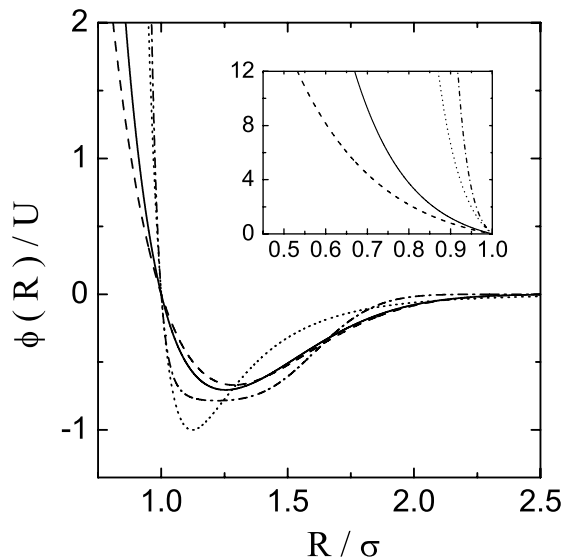


FIG. 1. Effective pair potentials analyzed in this paper. Reduced units r/σ and ϕ/U are used with appropriate values for σ and U for each model, as defined in the text. Full line: alkali-wis potential, ϕ_{Na} . Dash-dotted line: model for Hg, ϕ_{Hg} . Dotted line: Lennard-Jones potential. Dashed line: artificially softened version, ϕ_{soft} . The inset shows an enlarged view of the repulsive part of $\phi(R)$.

T_m/T_c and layering at the free liquid surface. In order to clarify the correlation between these two features we have added one more interaction model, which we call “soft alkali” and is also presented in Fig. 1. In this model the α parameter in the ϕ_{Na} is arbitrarily reduced to two-thirds times its original value, keeping the same values for R_1 and β , while A_0 and A_1 are changed to keep the values of σ and U .

Density functional calculations with these models give oscillatory liquid-vapor density profiles at low T as also observed in previous works [15]. However, the predicted melting temperature moves from above to below the onset of the oscillations, depending on the technical details of the approximation used, so that the theory cannot give a definite answer and we had to rely on computer simulations. To determine the bulk phase diagram for each interaction potential we first minimized the energy at $T = 0$; the equilibrium structure always has fcc symmetry. To locate the melting point, this structure is used as an input configuration for a series of NPT Monte Carlo simulations at zero pressure and increasing temperature. 864 particles were used with periodic boundary conditions; all potentials were truncated at 2.5σ . The open symbols in Fig. 2 show the equilibrium density at each temperature, and jumps indicate the position of the melting point at zero pressure, very close to the actual triple point given the small value of the vapor density at low T . We take the temperature at the jump as an upper limit to the true T_m in each case, so that the solid-liquid transition could appear at a lower temperature, but never above it. Thus, for LJ we get the value 0.76 well above the best estimates for $k_B T_m/\epsilon \approx 0.68$. To obtain the liquid-vapor phase diagrams at high temperature, and also the structure of the free liquid surface, we have

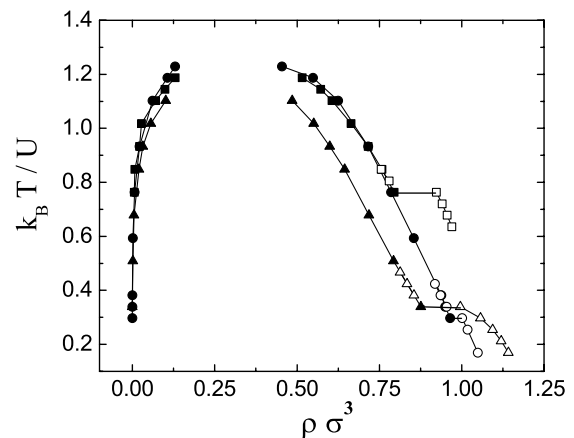


FIG. 2. Comparison of phase diagrams obtained with model potentials ϕ_{Na} (circles), ϕ_{Hg} (triangles), and ϕ_{LJ} (squares). Reduced temperature $k_B T/U$ and density $\rho \sigma^3$ are used with appropriate scaling constants U and σ for each potential model, as described in the text. The open symbols correspond to NPT Monte Carlo results at zero pressure. The closed symbols are results of the coexisting densities from NVT Monte Carlo simulations in slab geometry. The lines are guides to the eye.

carried out a series of *NVT*-MC simulations with 2592 particles in a rectangular box, periodically replicated in all three directions. Particles were arranged in slab geometry by dividing the central box into nine cubes of equal size along the z axis. The three inner cubes were filled with particles, the remaining six boxes being empty which creates two similar, flat interfaces in the system, with transverse sizes about 9σ . Below T_c the systems equilibrate to slabs of liquid, with vapor on both sides. Sampling times in excess of 3×10^5 MC steps were necessary to achieve equilibration. The results for the coexisting liquid-vapor densities are also shown in Fig. 2 (closed symbols).

The critical temperature obtained with the pair potential $\phi_{\text{Na}}(r)$ is $T_c \approx 1.22U_{\text{Na}}/k_B = 2669$ K, less than 8% above the experimental value for Na (2483 K), while $\phi_{\text{Hg}}(r)$ gives $T_c \approx 1.15U_{\text{Hg}}/k_B = 1686$ K, within 10% of the experimental value for Hg (1751 K). The agreement is quite satisfactory, considering the simplicity of our representation and the limited amount of information used to extract these effective pair potentials. The main conclusion from the phase diagrams is the remarkable differences in the ratio T_m/T_c , which is about 0.66 for the LJ potential, 0.24 for ϕ_{Na} , and 0.30 for ϕ_{Hg} . These latter values are still high compared with the experimental results for metals, reflecting the limited accuracy of our simple pair-potential model to incorporate the subtle many-body effects in real metals, but the qualitative effect of a low reduced melting temperature may certainly be obtained with these two simple pair potentials. It was difficult to guess the shape of a pair potential that gives a low T_m/T_c , and our use of a simple effective description of the two metals considered provided us with two particular forms of very different characteristics. The artificial enhancement of their features may help establish their relevance; for the alkalilike pair potential we find that the decrease in melting temperature is linked to the softness of the repulsive part. Using the artificially softened version (see Fig. 1) we obtain $k_B T_c/U \approx 1.3$ and a drop of T_m to $T_m/T_c \approx 0.13$, very similar to the experimental value for Hg. However, when the repulsive part is hardened (by artificial increase of the α parameter), the melting temperature increases to a ratio comparable to that for the LJ potential. Despite this result, the repulsive part of ϕ_{Hg} is harder than that of ϕ_{LJ} but it still has a lower T_m/T_c , so that another feature of ϕ_{Hg} (possibly its broad and flat well) is relevant.

Results for the liquid-vapor surface structure, shown in Fig. 3, were obtained from the same *NVT*-MC simulations (in slab geometry) used to obtain the liquid-vapor coexistence curve. The reported liquid-vapor density profiles are independent of the initial configuration of the slab (either liquid or solid), which gives a further check on equilibration, but in the *NVT* slab simulation melting is observed at slightly lower T than in the *NPT* MC. We present density profiles at three different temperatures for each pair-potential model. The lowest T is always that for which

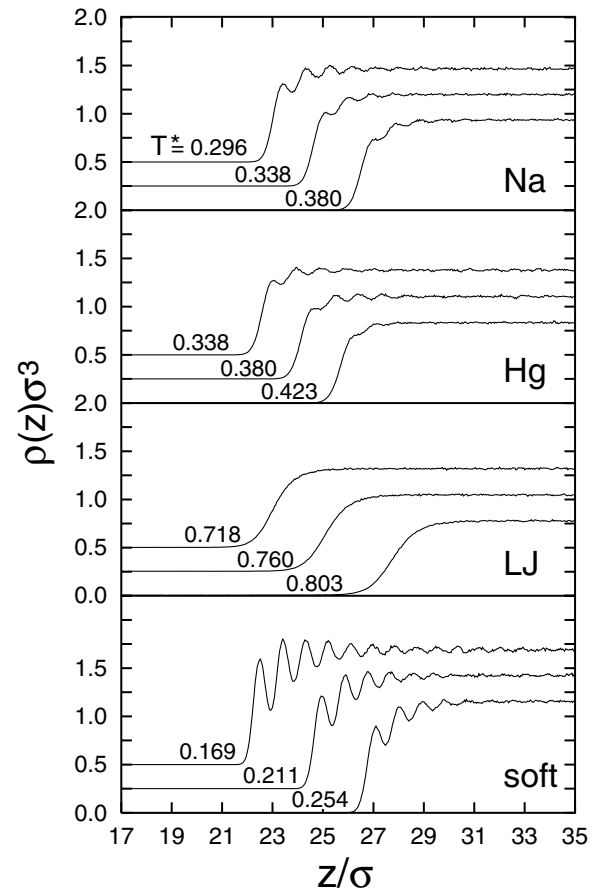


FIG. 3. Liquid-vapor density profiles in reduced units, z/σ and $\rho(z)\sigma^3$, for model potentials ϕ_{Na} , ϕ_{Hg} , ϕ_{LJ} , and ϕ_{soft} . The results in each case are for three values of $T^* = k_B T/U$ just above the melting point.

the crystal slab has already melted (but the crystal in the *NPT* simulation has not), the next profile corresponds to the first temperature for which the *NPT* bulk melting has been observed, and the third profile corresponds to a further increase of T .

Despite their different shapes, ϕ_{Na} and ϕ_{Hg} lead to similar density profiles (Fig. 3), with weak oscillatory structures damped as T grows. The lowest temperature in each case should be close to T_m , while the second and third are certainly above melting. Thus the weak but clearly visible density oscillation is not an artifact of having an overcooled metastable liquid. Surface layering is slightly stronger for ϕ_{Na} than for ϕ_{Hg} because of the small difference in reduced melting temperature, but comparison of the density profiles for the same values of reduced temperature in the two models shows a clear similarity.

The density profiles for the LJ model (Fig. 3) have the usual monotonic shape observed in many previous papers. Similar shapes are obtained for ϕ_{Na} and ϕ_{Hg} at the same values of reduced temperature. Then, the lack of oscillatory structure in the LJ model is due only to its high T_m , which precludes the study of the equilibrium liquid at lower

temperatures. We checked that cooling of the LJ liquid slab well below T_m generates oscillatory structures similar to those observed for the other pair potentials. However, the interpretation of such metastable states is subtle and they may be impossible to observe experimentally.

For the model potential ϕ_{soft} , with T_m/T_c similar to the experimental value for Hg, the profiles (Fig. 3) show very strong oscillations, which confirms the hypothesis that the crucial requirement to this effect is the low value of T_m/T_c . Again, the profiles given by ϕ_{soft} at higher T are very close to the profiles of the other models at similar values of T/U . We may compare these density profiles with those obtained by theoretical treatments of the different metals and with experimental results. The first peak in our layering structures is always lower than the second peak, in contrast with the usual interpretation of the experimental results [9,10] but in agreement with some previous theoretical calculations [16] and with simulations results for a liquid-liquid interface at high pressure [17]. This latter work analyzes the damping of the oscillations with increasing transverse areas, due to the capillary waves; in our case this effect should be reduced by the large surface tension and low T . Simulations with a 50% increase of the linear transverse size (up to 14σ) for ϕ_{soft} give very little change in the density profiles (too small to be seen at the scale of Fig. 3), which is consistent with the capillary wave prediction [17] using the surface tension of our model, $\gamma\sigma^2/k_B T \approx 8$ (similar to the experimental values for Hg). The relevant size for x-ray reflectivity experiments [9] is probably about 300σ and the damping effect would produce an appreciable reduction of the oscillations (approximately by a factor of 4) with respect to that observed with our simulation, but without change in our qualitative conclusion: fluids with realistic isotropic pairwise interactions (without kinks, shoulders, or double-well structures) exhibit layering at the liquid-vapor surface provided that the system has a low melting temperature relative to T_c . It seems likely that (at least part of) the explanation for surface layering does not require many-body interactions. Our results would predict strong surface layering in metals such as Hg, with low T_m/T_c ratio, and much weaker (or even absent) layering in metals such as Al and Mg, with higher T_m/T_c . Oscillations in the alkali metals, with intermediate values of T_m/T_c , would be at the limit of observation [18]. Within our analysis for the $\phi_{\text{Na}}(r)$ and $\phi_{\text{soft}}(r)$ models, this trend is consistent with the well-known re-

sults [13] that the repulsive part of the potentials for Al and Mg are harder than those for the alkalis. Further work is needed to understand the low value of T_m in the $\phi_{\text{Hg}}(r)$ model, and to explore the possible existence of systems other than metals in which the shape of the effective pair potential may lead to low melting temperatures and, according to our prediction, to strong liquid surface layering.

This work was supported by the Dirección General de Educación Superior e Investigación Científica of Spain, under Grants No. PB97-1223 and No. 1FD97-1358.

-
- [1] B. Ocko *et al.*, Phys. Rev. Lett. **57**, 94 (1986).
 - [2] Y. Martínez-Ratón, A. Somoza, L. Mederos, and D. Sullivan, Faraday Discuss. **104**, 111 (1996).
 - [3] R. Evans, in *Fundamentals of Inhomogeneous Fluids*, edited by D. Henderson (Dekker, New York, 1992), pp. 85–175.
 - [4] J. S. Rowlinson and B. Widom, *Molecular Theory of Capillarity* (Clarendon Press, Oxford, 1982); D. Beaglehole, in *Fluid Interfacial Phenomena*, edited by C. A. Croxton (Wiley, New York, 1986), pp. 523–554.
 - [5] G. Fabricius *et al.*, Phys. Rev. B **60**, R16283 (1999).
 - [6] S. Barton *et al.*, Nature (London) **321**, 685 (1986).
 - [7] J. Harris, J. Gryko, and S. A. Rice, J. Chem. Phys. **87**, 3069 (1987); M. Zhao, D. Chekmarev, Z. Cai, and S. A. Rice, Phys. Rev. E **56**, 7033 (1997).
 - [8] M. A. Gómez and E. Chacón, Phys. Rev. B **46**, 723 (1992); Phys. Rev. B **49**, 11 405 (1994); M. Hasegawa and M. Watabe, J. Phys. C **15**, 353 (1982).
 - [9] O. Nagnussen *et al.*, Phys. Rev. Lett. **74**, 4444 (1995); E. DiMasi *et al.*, Phys. Rev. B **58**, R13419 (1998).
 - [10] M. Regan *et al.*, Phys. Rev. Lett. **75**, 2498 (1995).
 - [11] F. Celestini, F. Ercolessi, and E. Tosatti, Phys. Rev. Lett. **78**, 3153 (1997); S. Iarlori, P. Carnevali, F. Ercolessi, and E. Tosatti, Surf. Sci. **211/212**, 55 (1989).
 - [12] Y. Li, E. Blaisten-Barojas, and D. A. Papaconstantopoulos, Phys. Rev. B **57**, 15 519 (1998).
 - [13] R. Kumaravadivel and R. Evans, J. Phys. C **9**, 3877 (1976).
 - [14] S. Munejiri, F. Shimojo, and K. Hoshino, J. Phys. Condens. Matter **10**, 4963 (1998).
 - [15] R. Evans *et al.*, Mol. Phys. **80**, 755 (1993).
 - [16] D. Chekmarev, M. Zhao, and S. A. Rice, J. Chem. Phys. **109**, 768 (1998).
 - [17] S. Toxvaerd and J. Stecki, J. Chem. Phys. **102**, 7163 (1995).
 - [18] H. Tostmann *et al.*, Phys. Rev. B **61**, 7284 (2000).